

三(三甲基硅烷)类添加剂助力5 V 镍锰酸锂电池实用化

张立恒¹ 顾海涛² 罗英² 董庆雨³ 沈炎宾^{*,3} 解晶莹^{*,1,2}

(¹哈尔滨工业大学化工与化学学院, 哈尔滨 150001)

(²上海空间电源研究所, 空间电源技术国家重点实验室, 上海 200245)

(³中国科学苏州纳米技术与纳米仿生研究所国际实验室卓越纳米科学中心, 苏州 215123)

摘要: 基于LiNi_{0.5}Mn_{1.5}O₄的5 V 电池尚未实现实际应用, 解决这一问题的关键在于电解液调控和电极界面优化。我们系统性研究了三(三甲基硅烷)硼酸酯(TMSB)和三(三甲基硅烷)亚磷酸酯(TMSPi)作为常规碳酸乙烯酯(EC)-LiPF₆基电解液添加剂在LiNi_{0.5}Mn_{1.5}O₄电池体系中的应用。结合理论计算、物理化学表征以及电化学手段分析了三(三甲基硅烷)类添加剂在高压电解液中的作用机制。研究发现, TMSB和TMSPi均可以通过优化电极/电解液界面来提高LiNi_{0.5}Mn_{1.5}O₄循环稳定性和库仑效率。TMSB中缺电子B可与阴离子相互作用, 稳定PF₆⁻, 抑制LiNi_{0.5}Mn_{1.5}O₄正极阻抗的持续增加。TMSPi具有更高的最高占据分子轨道(HOMO)能级, 可在更低电位下钝化高压正极, 提高LiNi_{0.5}Mn_{1.5}O₄放电电压平台和放电容量。此外, TMSPi还可通过亲核反应参与石墨界面组分优化, 改善负极循环性能。石墨||LiNi_{0.5}Mn_{1.5}O₄软包电池在含1% TMSPi电解液中1C循环100次后的容量保持率为88.9%, 优于基础电解液(60.5%)和含1% TMSB的电解液(77.4%)。

关键词: 电解液添加剂; LiNi_{0.5}Mn_{1.5}O₄; 三(三甲基硅烷)硼酸酯; 三(三甲基硅烷)亚磷酸酯

中图分类号: O646.21 **文献标识码:** A **文章编号:** 1001-4861(2022)10-2091-12

DOI: 10.11862/CJIC.2022.215

Tris(trimethylsilyl)-Based Additives Enables Practical 5 V LiNi_{0.5}Mn_{1.5}O₄ Batteries

ZHANG Li-Heng¹ GU Hai-Tao² LUO Ying² DONG Qing-Yu³ SHEN Yan-Bin^{*,3} XIE Jing-Ying^{*,1,2}

(¹School of Chemistry and Chemical Engineering, Harbin Institute of Technology, Harbin 150001, China)

(²State Key Laboratory of Space Power-Sources Technology, Shanghai Institute of Space Power-Sources, Shanghai 200245, China)

(³i-Lab, CAS Center for Excellence in Nanoscience, Suzhou Institute of Nano-Tech and Nano-Bionics, Chinese Academy of Sciences, Suzhou, Jiangsu 215123, China)

Abstract: LiNi_{0.5}Mn_{1.5}O₄ cathode materials have been considered promising candidates for high energy density Li-ion batteries due to their high operation potential. However, to develop 5 V LiNi_{0.5}Mn_{1.5}O₄-based batteries, practical electrolytes with high electrochemical stability are yet to be realized. In this work, tris(trimethylsilyl)-based additives, including tris(trimethylsilyl)borate (TMSB) and tris(trimethylsilyl)phosphite (TMSPi), were selected as electrolyte additives for typical ethylene carbonate (EC)-LiPF₆ based electrolyte to develop practical LiNi_{0.5}Mn_{1.5}O₄-based batteries. Combining theoretical calculations, physicochemical characterization, and electrochemical measurements, we found that both TMSB and TMSPi can improve the Coulombic efficiency and cycling stability of 5 V LiNi_{0.5}Mn_{1.5}O₄-based cells. Specifically, TMSB can act as the stabilizer for PF₆⁻ due to its electron deficiency nature, thereby suppressing the increase of cell impedance. In addition, thanks to its high highest occupied molecule orbital (HOMO) energy level, TMSPi can be preferentially oxidized on the surface of charged LiNi_{0.5}Mn_{1.5}O₄ electrodes, resulting in a decent rate capacity and high discharge platform. In addition, TMSPi is conducive to the formation of

收稿日期: 2022-07-09. 收修改稿日期: 2022-08-29.

国家自然科学基金(No. 21805186, 21625304, 21733012)、上海启明星项目(No. 20QB1401700)和上海科学技术委员会项目(No. 19160760700)资助。

*通信联系人。E-mail: jyxie@hit.edu.cn, ybshen2017@sinano.ac.cn

robust solid electrolyte interphase (SEI) on graphite anode through the nucleophilic attack, resulting in enhanced cycle performance. As a result, Graphite||LiNi_{0.5}Mn_{1.5}O₄ pouch cells with TMSPi-containing electrolyte displayed capacity retention of 88.9% after 100 cycles at 1C, superior to that in the blank (60.5%) and TMSB-containing (77.4%) electrolytes.

Keywords: electrolyte additive; LiNi_{0.5}Mn_{1.5}O₄; tris(trimethylsilyl)borate; tris(trimethylsilyl)phosphite

0 Introduction

High energy density, better safety, and low price of the next generation lithium-ion battery (LIB) are expected for power energy storage systems by continually optimizing these existing battery chemistries^[1-5]. Cathode materials with higher operating voltage can further increase their energy density than the ones with high discharge capacity alone^[6-7]. So far, numbers of cathode materials with high discharge platforms have been reported^[8-11]. One of the representatives is spinel LiNi_{0.5}Mn_{1.5}O₄ owing to its high lithium-ion utility ratio, safety, superior rate capability, and high discharge platform of 4.7 V (vs Li/Li⁺)^[12-13]. However, its practical application in commercial cells is still confronting several challenges, such as low Coulombic efficiency (CE) and poor cyclability^[14-18], which is essentially caused by catalytic and oxidative decomposition of electrolyte components on the surface of charged LiNi_{0.5}Mn_{1.5}O₄ electrodes^[19]. Nowadays, numerous studies have shown that functional additives can improve interface stability and cycle performance^[20]. Among those additives, siloxanes-based additives are widely investigated to relieve the decomposition of electrolyte components and suppress the self-discharge behavior of LiNi_{0.5}Mn_{1.5}O₄ electrodes by building a protective layer, such as tris(trimethylsilyl)borate (TMSB) and tris(trimethylsilyl)phosphite (TMSPi)^[21-27]. Their trimethylsilyl groups display high HF-scavenging ability, contributing to enhancing the stability of interface layers and inhibiting the dissolution of transition metal ions from the bulk cathodes. However, their comparative evaluations in practical LiNi_{0.5}Mn_{1.5}O₄-based cells and the difference of effect mechanism in LiPF₆-based electrolyte have not been reported systematically. It is also unclear how the central atom of tris(trimethylsilyl)-

based additive affects the interface properties of high-voltage cathode and graphite anode in practical application.

This work provides a comparative study on TMSB and TMSPi alone as electrolyte additives for LiNi_{0.5}Mn_{1.5}O₄ electrodes. Combining density functional theory (DFT) computation and electrochemical characterization, the possible mechanism of TMSB and TMSPi in ethylene carbonate (EC)-LiPF₆-based electrolytes was systematically explored. Meanwhile, their effect on graphite anode and the pouch cells was also concerned in this work.

1 Experimental

1.1 Electrolyte and electrode preparation

The baseline electrolyte (BE) composed of 1.2 mol·L⁻¹ LiPF₆ and EC/ethyl methyl carbonate (EC/EMC, 3:7, V/V) was purchased from DoDoChem (China, H₂O content: *ca.* 8.4 mg·L⁻¹). 1% TMSB and 1% TMSPi (TCI chemicals, 99%) were introduced to the BE and stored for 24 h in an argon-filled glovebox (PRS226/S10-0963, H₂O content < 0.1 mg·L⁻¹) to follow-up measurement.

To evaluate the electrochemical performance of the BE and additives-containing electrolytes, 2025-type coin cells and 0.5 Ah Graphite||LiNi_{0.5}Mn_{1.5}O₄ pouch cells were fabricated. The cathode was prepared by coating the mixture LiNi_{0.5}Mn_{1.5}O₄ powders (XingNeng New Materials Co., Ltd.), Super P (Amerys), and polyvinylidene fluoride (PVDF, HSV900, Solvay) (mass ratio of 90:5:5) onto Al current collector with mass loading of 22.0 mg·cm⁻². For coin cells, the areal mass loading was 4.0 mg·cm⁻². The anode was prepared by coating the mixture of graphite (G25, Shanshan Tech Co., Ltd.), Super P, sodium carboxymethyl cellulose (CMC, Walocel CRT2000 PPA12,

Dow Wolff Cellulosics®), and styrene butadiene rubber (SBR, Lipaton SB5521, Synthomer) (mass ratio of 93:2:2:3) on the Cu foil. For coin cells and pouch cells, the areal mass loading of the graphite electrode was $9.0 \text{ mg} \cdot \text{cm}^{-2}$. The 0.5 Ah pouch cells were designed and assembled with the negative/positive area-capacity ratio (N/P) of *ca.* 1.18 (according to the calculation with $130 \text{ mAh} \cdot \text{g}^{-1}$ for cathodes and $330 \text{ mAh} \cdot \text{g}^{-1}$ for graphite anode) in the drying room. The Celgard 2325 separator was used in all these cells.

1.2 Electrochemical measurement

Charge - discharge tests were performed on the LAND test system (CT 2001A) with a voltage range of 3.5-5.0 V for $\text{Li}|\text{LiNi}_{0.5}\text{Mn}_{1.5}\text{O}_4$ coin cells and 3.5-4.9 V for Graphite $|\text{LiNi}_{0.5}\text{Mn}_{1.5}\text{O}_4$ pouch cells. Electrochemical impedance spectra (EIS) were obtained on VMP-300 electrochemical workstation (Bio - Logic) with a voltage amplitude of 10 mV and a frequency range of 5 MHz-0.1 Hz. The electrochemical behaviors of electrolytes were also examined by linear sweep voltammetry (LSV) test using Li|Al coin cell at a scan rate of $0.1 \text{ mV} \cdot \text{s}^{-1}$. For cyclic voltammetry (CV) measurements, the experiments were also conducted on VMP - 300 using $\text{Li}|\text{LiNi}_{0.5}\text{Mn}_{1.5}\text{O}_4$ coin cells with a potential range from the open circuit voltage (OCV) to 6.0 V at a scan rate of $0.1 \text{ mV} \cdot \text{s}^{-1}$.

1.3 Characterization

The ionic conductivities of the electrolytes were measured by a METTLER TOLEDO Seven Direct SD30 (Inlab 710 electrode). The electrode morphology was collected by scanning electron microscope (SEM, S4800, Hitachi, Japan) operated at 5 kV. The interface layers were observed by transmission electron microscope (TEM, JEOL JEM-2100F) operated at 200 kV. The X - ray diffraction (XRD) patterns of fresh and cycled electrodes were collected on a Bruker D8 Advance (Germany) diffractometer at a scan rate of $5 \text{ (}^\circ\text{)} \cdot \text{min}^{-1}$ and the range of 10° - 80° using Cu $K\alpha$ radiation with $\lambda=0.15148 \text{ nm}$ under 40 kV and 40 mA. The X-ray photoelectron spectroscopy (XPS) was carried out on AXIS-ULTRA DLD-600W (SHIMADZU-KRATOS. Co., Ltd.) to assess the interface composition of cycled electrodes, and the pass energy was fixed at 30.0 eV.

Inductively coupled plasma (ICP) tests were conducted by the Thermofisher iCAP-7200 Duo instrument. Importantly, before the SEM, TEM, XRD, ICP, and XPS analysis, cycled electrodes were rinsed with pure dimethyl carbonate (DMC) to remove superfluous electrolyte and dried for 12 h at 50 °C in an argon-filled glove box, then stored in the bottles for the subsequent tests.

1.4 Theoretical calculations

Geometry optimization of molecules was executed by the Dmol³ module in Material Studio Software. A frequency analysis was obtained at DFT. Moreover, the relative Gibbs free energy was calculated at 298.15 K.

2 Results and discussion

2.1 Reactivity of selected additives in EC-LiPF₆-based electrolyte

HOMO energy level based on the molecular orbital theory has been widely adopted to predict the oxidation tendency of organic molecules^[28]. According to DFT calculation results, as shown in Fig. 1a, TMSB and TMSPi are prone to lose electrons for their high HOMO (-7.70 and -6.26 eV , respectively) relative to EC (-8.31 eV) and EMC (-7.96 eV). Therefore, they can be preferentially oxidized and contribute to the formation of protective film on the charged $\text{LiNi}_{0.5}\text{Mn}_{1.5}\text{O}_4$ electrodes. LSV tests were adopted with Li|Al cells from OCV to 5.5 V (vs Li/Li⁺) at a scan rate of $0.1 \text{ mV} \cdot \text{s}^{-1}$ to evaluate the oxidation potential and electrochemical reactivity of additives. As shown in Fig. 1b, the LSV curves showed that TMSB began to be oxidized over 3.7 V (vs Li/Li⁺) with relatively high oxidation current as the potential increase, displaying higher reactivity under high voltage, which may affect the initial CE of cells. By contrast, TMSPi appeared to be oxidized at a lower potential though the oxidation current was relatively small, displaying a higher electrochemical window, indicating that TMSPi had a faster film-passivating ability at comparatively low potential than TMSB. The CV result in Fig. S1 (Supporting information) is consistent with the above conclusions.

Moreover, TMSB and TMSPi, especially for TMSPi, display high reactivity with HF molecule via

the P—O and O—Si cleavage reaction, as shown in Fig. 2, which is in good harmony with the report about the HF-scavenging ability of TMSPi in EC-LiPF₆ based electrolyte^[29-30]. Similarly, the reactions of TMSB or TMSPi with LiF via the O—Si bond cleavage are ther-

modynamically favorable. Moreover, electron deficiency of B in TMSB also displays a high affinity with F⁻, as shown in Fig. S2, which can reasonably accelerate the dissolution of LiF in interface layers, resulting in reduced interface impedance among cycling.

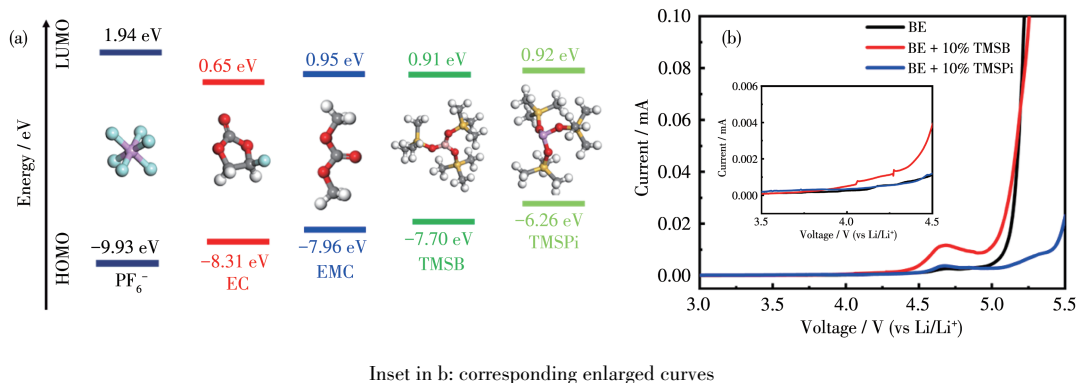


Fig. 1 (a) Chemical structure and its HOMO/LUMO energy level of PF₆⁻ and organic molecules; (b) LSV curves from OCV to 5.5 V (vs Li/Li⁺) at a scan rate of 0.1 mV·s⁻¹ in different electrolytes

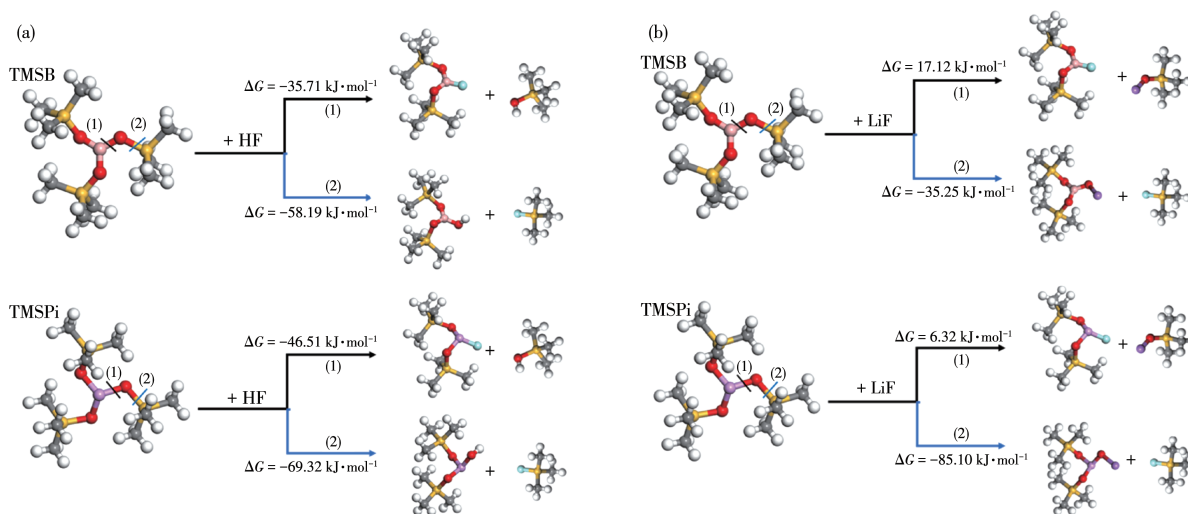


Fig. 2 Reaction energies (ΔG in kJ·mol⁻¹) of TMSB and TMSPi with HF (a) or LiF (b) molecule by Dmol³ module

2.2 Electrochemical performance of Li||LiNi_{0.5}Mn_{1.5}O₄ electrode

Fig. 3 shows the cycling stability of Li||LiNi_{0.5}Mn_{1.5}O₄ coin cells in BE and additive-containing electrolytes at 1C and 25 °C after precycling at 0.2C for three cycles. The 1% addition (mass fraction) was decided by the reported literature^[22]. LiNi_{0.5}Mn_{1.5}O₄ electrodes in additive-containing electrolytes showed excellent cycling stability, without noticeable capacity fading over 200 cycles. Its capacity-retention was improved from 85.9% (BE, average CE of 99.2%) to 92.3% (TMSB-containing electrolyte) and 95.1% (TMSPi-containing

electrolyte) along with an enhanced CE of 99.4%. It is worth noting that there exists sharp capacity fading in BE after 150 cycles, mainly due to the massive consumption of electrolytes on the surface of LiNi_{0.5}Mn_{1.5}O₄ and the breakdown of the electrically conductive network^[31]. Significantly, both TMSB and TMSPi can hinder the capacity fading of LiNi_{0.5}Mn_{1.5}O₄, suggesting that two selected additives can effectively stabilize the cathode/electrolyte interface and relieve the decomposition of electrolyte components. Moreover, as shown in Fig. 3a and 3f, LiNi_{0.5}Mn_{1.5}O₄ electrode in TMSPi-containing electrolyte exhibited a higher discharge plat-

form and specific capacity with lower polarization (Fig. 3c) than that in BE or TMSB-containing electrolyte, suggesting that TMSPi-derived cathode interface layer (CEI) exhibits faster kinetics of the charge transfer on the surface of the $\text{LiNi}_{0.5}\text{Mn}_{1.5}\text{O}_4$ electrodes^[27,29]. The medium-voltage of the $\text{LiNi}_{0.5}\text{Mn}_{1.5}\text{O}_4$ electrode during cycling is displayed in Fig. 3b. Clearly, its discharge platform kept dropping during cycling in BE, mainly ascribing to the increased cell impedance^[31]. Surprisingly, both two selected additives can effectively hinder the platform voltage dropping, especially for TMSPi-containing electrolytes, as shown in Fig. 3b and 3d-3f. The results show that $\text{LiNi}_{0.5}\text{Mn}_{1.5}\text{O}_4$ in TMSPi-containing electrolyte can maintain a higher discharge platform than others during cycles, which may mainly

be due to its low impedance and fast Li^+ transport in this phosphate-containing protective layers.

The resistance changes of $\text{LiLiNi}_{0.5}\text{Mn}_{1.5}\text{O}_4$ cells before and after cycling in different electrolytes are shown in Fig. 4. EIS curves of $\text{LiNi}_{0.5}\text{Mn}_{1.5}\text{O}_4$ mainly comprise electrolyte resistance (R_s), interfacial resistance (R_{SEI}), charge transfer resistance (R_{ct}), and Li^+ diffusion (W_p , a slop line at low frequency) in electrode^[32]. Table 1 shows the corresponding fitting data of R_{SEI} and R_{ct} . The result indicates that R_{SEI} of $\text{LiNi}_{0.5}\text{Mn}_{1.5}\text{O}_4$ electrode after 200 cycles in BE was higher than that of additive-containing electrolytes, resulting from the oxidative decomposition of electrolyte components. Above all, R_{SEI} and R_{ct} before and after 200 cycles in additive-containing electrolytes had no obvious change, reveal-

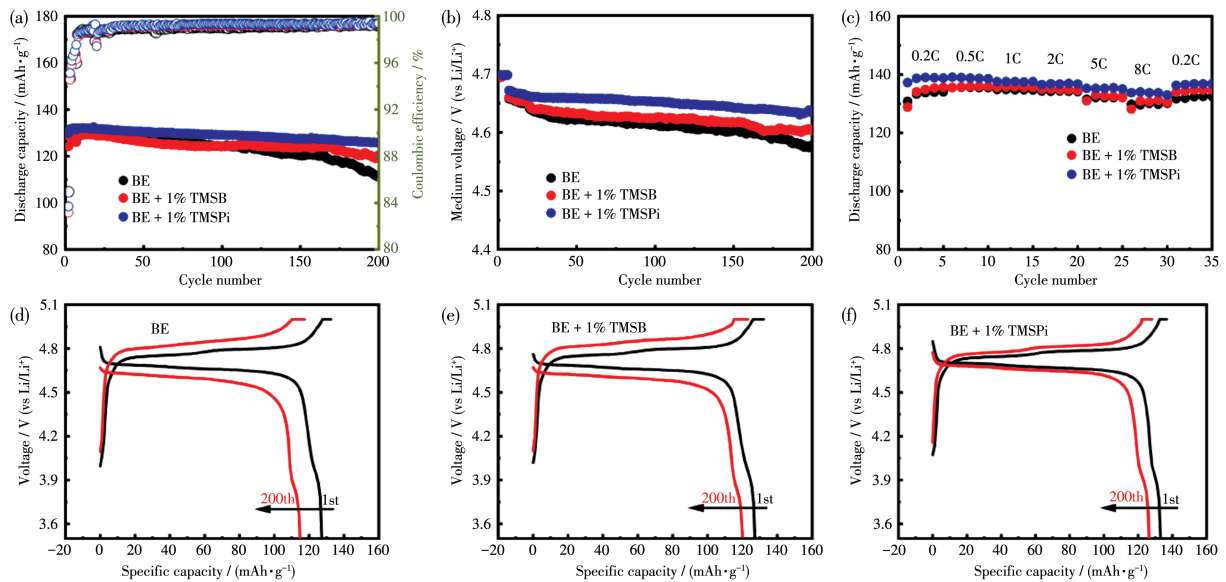


Fig.3 (a) Cyclic performance and (b) medium voltages of $\text{LiLiNi}_{0.5}\text{Mn}_{1.5}\text{O}_4$ half cells in different electrolytes at 1C; (c) Rate capability of $\text{LiLiNi}_{0.5}\text{Mn}_{1.5}\text{O}_4$ half cells in different electrolytes; (d-f) Charge-discharge curves of $\text{LiLiNi}_{0.5}\text{Mn}_{1.5}\text{O}_4$ half cells at 1C before and after 200 cycles in BE and additive-containing electrolytes

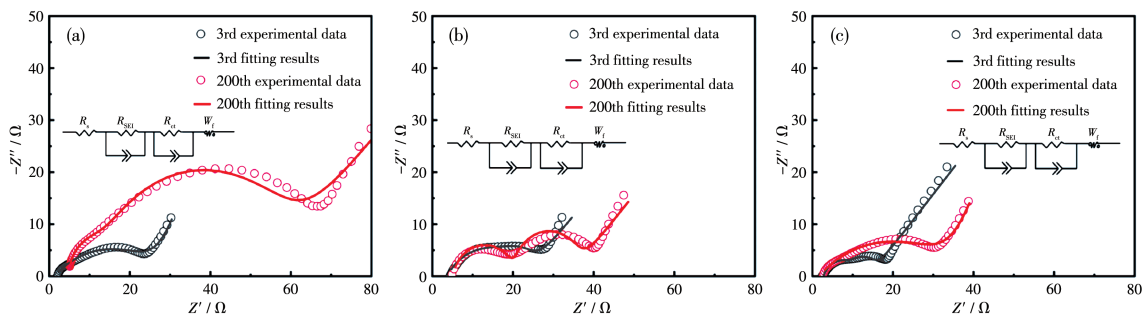


Fig.4 EIS spectra and fitting results of the $\text{LiLiNi}_{0.5}\text{Mn}_{1.5}\text{O}_4$ half cells before and after 200 cycles in BE (a), TMSB-containing (b), and TMSPi-containing (c) electrolytes at 1C and 25 °C

ing the electrically conductive network and interface layers of $\text{LiNi}_{0.5}\text{Mn}_{1.5}\text{O}_4$ electrodes remain stable during cycling. Significantly, R_{SEI} of $\text{LiNi}_{0.5}\text{Mn}_{1.5}\text{O}_4$ electrode in TMSB-containing electrolyte after 200 cycles was slightly decreased, mainly owing to the strong affinity of B with F^- and PF_6^- , leading to the dissolution of LiF and stabilization of electrolytes. While $\text{LiNi}_{0.5}\text{Mn}_{1.5}\text{O}_4$ electrodes in TMSPi-containing electrolyte show the lowest initial cell impedance, conducive to its high discharge platform.

Table 1 Fitting resistances of the cycled $\text{LiNi}_{0.5}\text{Mn}_{1.5}\text{O}_4$ cells in different electrolytes

| Sample | R_{SEI} / Ω | R_{ct} / Ω |
|-------------|---------------------------|--------------------------|
| BE-5th | 10.9 | 15.5 |
| BE-200th | 20.8 | 47.4 |
| TMSB-5th | 12.1 | 16.3 |
| TMSB-200th | 12.5 | 22.6 |
| TMSPi-5th | 6.3 | 10.4 |
| TMSPi-200th | 10.4 | 20.7 |

Though the above work has suggested that low mass loading ($4.0 \text{ mg}\cdot\text{cm}^{-2}$) and excessive electrolyte can support the $\text{LiNi}_{0.5}\text{Mn}_{1.5}\text{O}_4$ cells to achieve acceptable cycle performance in BE or additive-containing electrolytes, it has no clear distinction between the passivating ability of additives on the surface of $\text{LiNi}_{0.5}\text{Mn}_{1.5}\text{O}_4$ electrodes. Complex factors include oxidative decomposition of electrolyte components, the breakdown of electrically conductive networks, and others, all of which can cause the fading of battery performance. Conversely, with high mass loading and short cycles, the capacity degradation of

$\text{LiNi}_{0.5}\text{Mn}_{1.5}\text{O}_4$ cells is mainly derived from the oxidative decomposition of electrolyte components. As shown in Fig. S3, the $\text{LiNi}_{0.5}\text{Mn}_{1.5}\text{O}_4$ electrodes ($22.0 \text{ mg}\cdot\text{cm}^{-2}$) in BE suffered severe capacity fading after 50 cycles at 0.5C with a low CE of 98.7%, resulting from the massive decomposition of electrolyte components. Significantly with selected additives, the cycling stability of $\text{LiNi}_{0.5}\text{Mn}_{1.5}\text{O}_4$ was dramatically enhanced, especially for TMSPi with a high CE of 99.4%. It can be inferred that the ability of TMSPi on passivating the $\text{LiNi}_{0.5}\text{Mn}_{1.5}\text{O}_4$ electrode interface is superior to TMSB.

2.3 Morphology and interface layer of the $\text{LiNi}_{0.5}\text{Mn}_{1.5}\text{O}_4$ electrode

Fig. 5 shows the morphology and interface layer of the fresh and cycled $\text{LiNi}_{0.5}\text{Mn}_{1.5}\text{O}_4$ electrode. Different from the fresh electrode, the surface of $\text{LiNi}_{0.5}\text{Mn}_{1.5}\text{O}_4$ particles after cycling in BE is covered with amorphous products, mainly resulting from the oxidative decomposition products of electrolyte components and binders^[20,33]. Few amorphous products were found on the surface of $\text{LiNi}_{0.5}\text{Mn}_{1.5}\text{O}_4$ electrodes after cycling in additive-containing electrolytes, as shown in Fig. 5c-5d, indicating both TMSB and TMSPi can effectively relieve this decomposition reaction. Moreover, TEM results showed a similar thickness of interface layer on the surface of $\text{LiNi}_{0.5}\text{Mn}_{1.5}\text{O}_4$ particle after cycling in additive-containing electrolytes (2-3 nm), which is thinner and more uniform than that in BE (15-20 nm). Despite, the surface of $\text{LiNi}_{0.5}\text{Mn}_{1.5}\text{O}_4$ electrode after cycling in TMSPi-containing electrolyte (Fig. 5d and 5h) was not smooth as that in TMSB-containing electro-

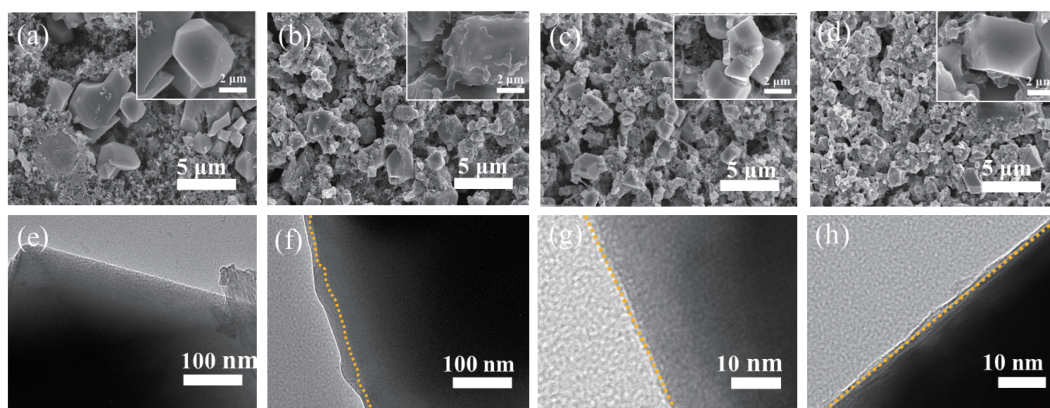


Fig. 5 SEM and TEM images of the fresh $\text{LiNi}_{0.5}\text{Mn}_{1.5}\text{O}_4$ (a, e) and $\text{LiNi}_{0.5}\text{Mn}_{1.5}\text{O}_4$ after 200 cycles in BE (b, f), TMSB-containing (c, g), and TMSPi-containing (d, h) electrolytes

lyte, existing a few discernible amorphous products, mainly due to the trace deposition of by-product from the high chemical reactivity of TMSPI with LiPF_6 .

2.4 Change of crystal structure for the $\text{LiNi}_{0.5}\text{Mn}_{1.5}\text{O}_4$ electrode

The crystal structure changes of the pristine and cycled $\text{LiNi}_{0.5}\text{Mn}_{1.5}\text{O}_4$ are shown in Fig. S4. Compared with the fresh electrodes, the main diffraction peaks of $\text{LiNi}_{0.5}\text{Mn}_{1.5}\text{O}_4$ electrodes at (311) and (400) were weakened after 200 cycles in BE. Surprisingly, the intensities of main diffraction peaks of $\text{LiNi}_{0.5}\text{Mn}_{1.5}\text{O}_4$ electrodes after cycling in additive-containing electrolytes keep strong, indicating that the selected additives can protect the crystal structure from disintegrating for long-term cycling. Especially for TMSPI-containing electrolytes, the XRD patterns of the cycled $\text{LiNi}_{0.5}\text{Mn}_{1.5}\text{O}_4$ electrode showed higher intensity among them, indicating TMSPI is more beneficial to the structural stability of $\text{LiNi}_{0.5}\text{Mn}_{1.5}\text{O}_4$.

Elemental analysis of $\text{Li}||\text{LiNi}_{0.5}\text{Mn}_{1.5}\text{O}_4$ cells after 200 cycles was performed by ICP tests on the Li metal anode, as shown in Fig.6. Significant Mn was deposited on the lithium metal anode after cycling in BE. However, with the selected additives, the Mn concentration was greatly reduced, especially for TMSPI-containing electrolytes. Therefore, both two additives can effectively prevent the dissolution of transition metal from the bulk $\text{LiNi}_{0.5}\text{Mn}_{1.5}\text{O}_4$ and stabilize its crystal structure. Significantly, TMSPI does much better than TMSB, which is in line with XRD data.

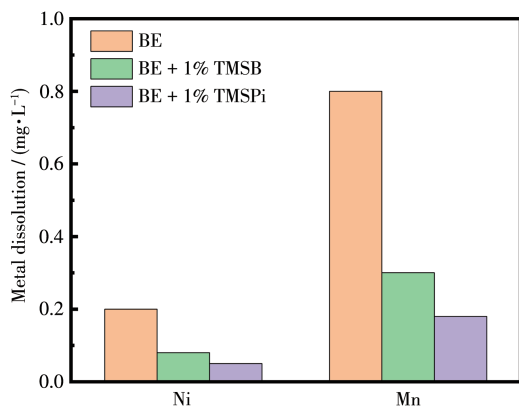


Fig.6 ICP results about Mn and Ni concentration on Li metal anode after 200 cycles

2.5 Surface compositions of the $\text{LiNi}_{0.5}\text{Mn}_{1.5}\text{O}_4$ electrode

The analysis of surface compositions was identified by XPS. As shown in Fig.7, the $\text{P}2p$, $\text{F}1s$, $\text{O}1s$, and $\text{C}1s$ spectra of the $\text{LiNi}_{0.5}\text{Mn}_{1.5}\text{O}_4$ electrodes after 200 cycles in different electrolytes. In the $\text{P}2p$ spectra, the peaks of Li_xPF_y (136.7 eV) and $\text{Li}_x\text{PO}_y\text{F}_z$ (134.1 eV) represent the decomposition products of LiPF_6 and they were reduced in TMSB-containing electrolyte. This result is consistent with $\text{F}1s$ spectra (Li_xPF_y), indicating the addition of TMSB can suppress the decomposition of the LiPF_6 . It may owe to the electron-withdrawing of boron acting as a stabilizer for LiPF_6 . Moreover, the trimethylsilyl group can react with HF and LiF to form a strong Si—F bond, reducing the content of high resistance of LiF. The peak at about 529.6 eV in $\text{O}1s$ spectra is attributed to metal—O (M—O) in $\text{LiNi}_{0.5}\text{Mn}_{1.5}\text{O}_4$. For the $\text{LiNi}_{0.5}\text{Mn}_{1.5}\text{O}_4$ electrodes after cycling in additive-containing electrolytes, the intensity of M—O is considerably stronger than that in BE, indicating a thinner surface film is formed in additive-containing electrolytes, which is in line with TEM data. Besides that, the peak corresponding to C—O (533.6 eV) and C=O (531.7 eV) in $\text{O}1s$ spectra correspond with the $\text{C}1s$ spectra (Fig.7d). The C—O bond, mainly caused by the decomposition of organic carbonate solvents, is slightly weakened in the additive-containing electrolytes, suggesting the decomposition of the electrolyte can be relieved by adding additives. Moreover, the C—Si bond was detected in the $\text{C}1s$ spectra on the $\text{LiNi}_{0.5}\text{Mn}_{1.5}\text{O}_4$ surface with TMSB-containing electrolyte, which is a benefit to forming a more stable Si-rich protective film^[34].

2.6 Effect of the selected additives on graphite electrode

For its practical application of additive-containing electrolytes in full cells, the effect of additives on the anode should not be overlooked. The $\text{Li}||\text{Graphite}$ cells were assembled with BE and additive-containing electrolytes. Fig. 8a shows the initial discharge/charge curves of $\text{Li}||\text{Graphite}$ cells at 0.1C. Obviously, the discharge curve of the graphite electrodes in TMSB-containing electrolytes almost coincided with that in BE. When cycling in TMSPI-containing electrolyte, the

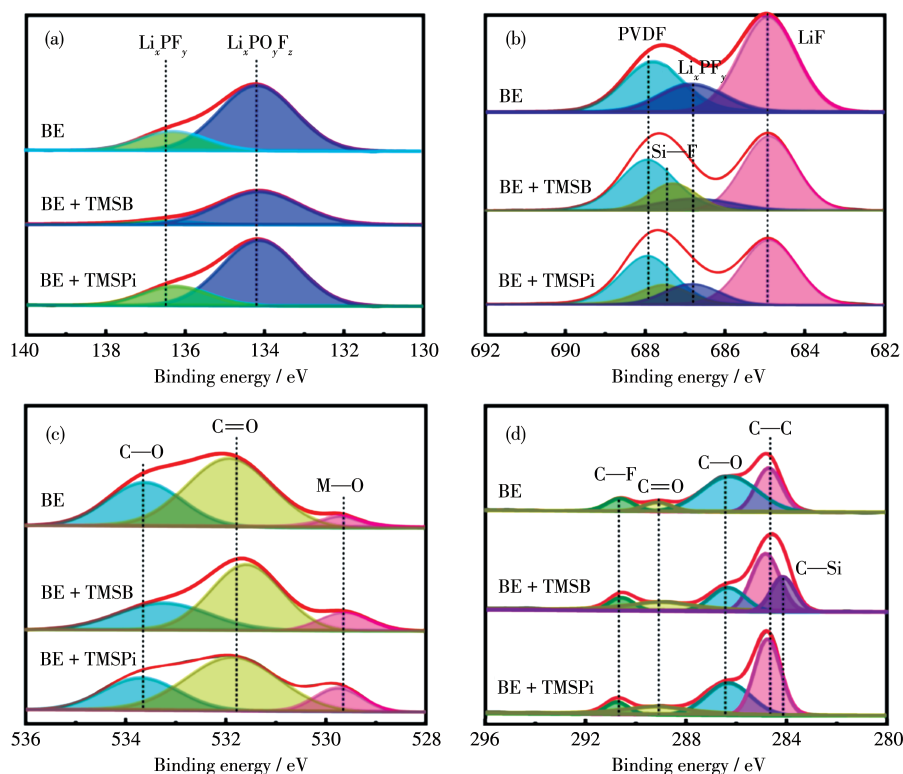


Fig.7 XPS spectra of the CEI layer of the $\text{LiNi}_{0.5}\text{Mn}_{1.5}\text{O}_4$ cathodes in different electrolytes after 200 cycles at 1C; (a) $\text{P}2p$, (b) $\text{F}1s$, (c) $\text{O}1s$, and (d) $\text{C}1s$

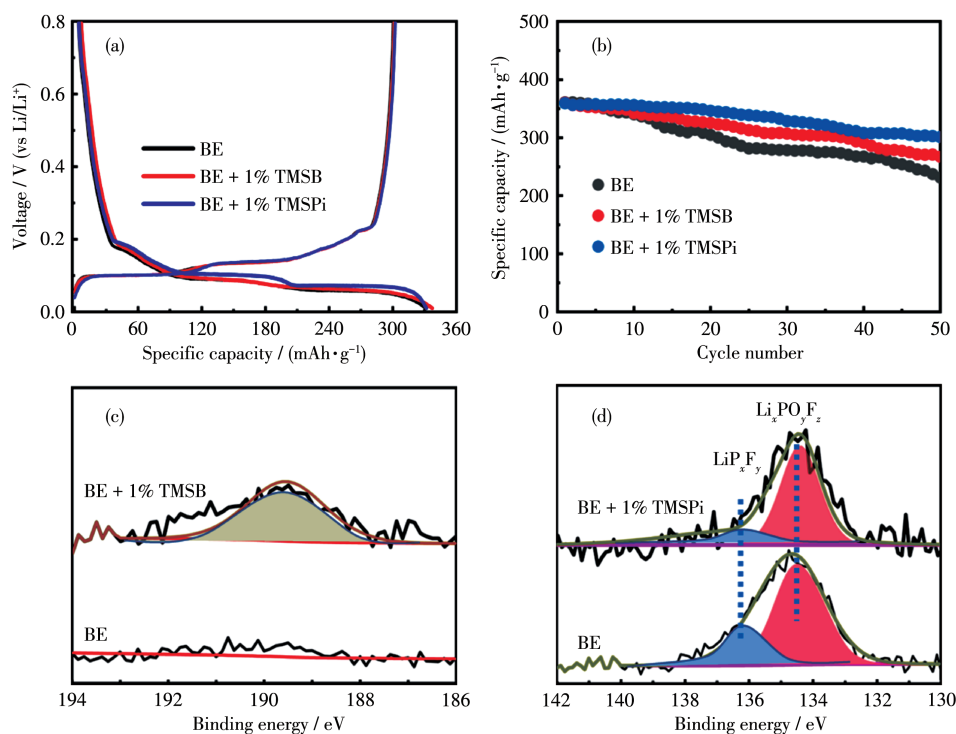


Fig.8 (a) Initial charge and discharge curves and (b) cycle performance of the graphite anodes in BE and additive-containing electrolytes; (c) $\text{B}1s$ XPS spectra of the graphite anodes after 50 cycles in BE and TMSB-containing electrolytes; (d) $\text{P}2p$ XPS spectra of the graphite anodes after 10 cycles in BE and TMSPi-containing electrolytes

LillGraphite cells showed a highest discharge platform and a lowest onset charge potential (0.043 V (vs Li/Li⁺)) than BE (0.061 V (vs Li/Li⁺)) and TMSB-containing electrolyte (0.051 V (vs Li/Li⁺)). It reveals that the selected additives are more conducive to decreasing the cell polarization of graphite anode, especially for TMSPi. Moreover, the TMSB/TMSPi-containing electrolytes, especially for TMSPi, can efficiently improve the electrochemical performance of LillGraphite cells, as shown in Fig. 8b. More borate or phosphate-containing species were also detected from the surface of graphite anode in the additives-containing electrolyte (Fig. 8c, 8d), which is beneficial to Li⁺ transportation. However, theoretical calculation showed that TMSB (0.91 eV) and TMSPi (0.92 eV) had higher LUMO values than EC (0.65 eV), indicating that they are difficult to be reduced in presence of EC via the electrochemical reaction on a graphite surface. Yim et al. has proved that the spontaneous decomposition reactions for neutral or cation state TMSPi and TMSB are thermodynamically forbidden^[35]. However, it is highly likely to undergo attack by nucleophiles (CH₃O⁻) on the graphite anode surface to participate in the SEI layer when TMSPi and EC coexist. The calculation results in Fig.

S5 showed that the Li⁺ affinity was greater for TMSPi than for EC, indicating TMSPi is likely to form an association with Li⁺ in the presence of EC. It is thermodynamically favorable for Li⁺-TMSPi and CH₃O⁻ to react via O—Si bond cleavage, leading to the formation of ((CH₃)₃SiO)₂POLi and (CH₃)₃SiOCH₃, participating in the formation of SEI layer on a graphite electrode.

2.7 Cycling stability of Graphite||LiNi_{0.5}Mn_{1.5}O₄ pouch cells

0.5 Ah Graphite||LiNi_{0.5}Mn_{1.5}O₄ pouch cells were fabricated to evaluate the comprehensive effects of selected additives on practical application, as shown in Fig. 9. In the first precycling process at 0.1C, the cells delivered an initial CE of 83.08% (BE), 81.23% (TMSB), and 82.85% (TMSPi) with a discharge capacity of about 0.55, 0.54, and 0.55 Ah respectively, indicating that TMSPi is more helpful to improve its energy density of pouch cells along with low initial cell impedance (Fig. 9c). Upon cycling at 1C (500 mA) and 25 °C, the pouch cells in BE suffer from rapid capacity fading, with only 60.5% of capacity retention after 100 cycles, as shown in Fig. 9d. Encouragingly, the cells with selected additives displayed relatively high retention (88.9% for TMSPi, 77.4% for TMSB, respectively).

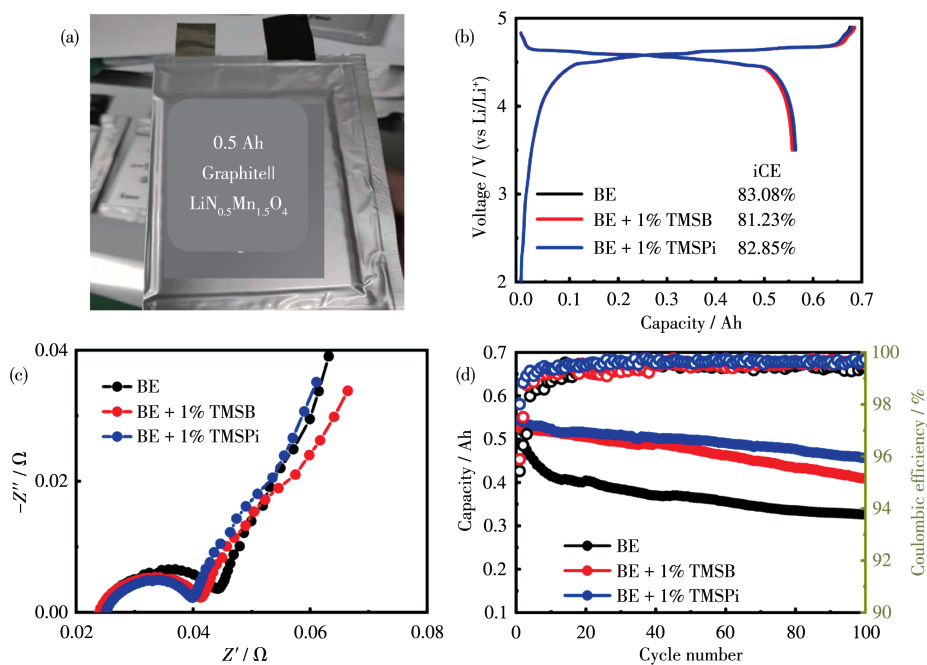


Fig. 9 (a) Image of 0.5 Ah Graphite||LiNi_{0.5}Mn_{1.5}O₄ pouch cells, (b) initial charge-discharge curves at 0.1C, (c) cell impedance, and (d) cycle performance at 1C in BE and additive-containing electrolytes

Hence, the capability of TMSPi on enhancing cycle performance for $\text{LiNi}_{0.5}\text{Mn}_{1.5}\text{O}_4$ was superior to TMSB. Besides that, the CE during cycling is another important indicator for $\text{LiNi}_{0.5}\text{Mn}_{1.5}\text{O}_4$ electrode-based cells^[36]. The main fading mechanism and low CE of $\text{LiNi}_{0.5}\text{Mn}_{1.5}\text{O}_4$ electrode are the oxidation decomposition reactions of electrolyte components^[19]. A relatively high CE of cells with functional additives indicates that these parasitic reactions have been effectively suppressed. Compared to the cells in BE (an average CE of 99.3%), the CE of pouch cells with TMSB and TMSPi can reach 99.5% and 99.6% in the first 30 cycles and remain stable in the following cycles. Consequently, TMSPi is a promising and better-selected additive than TMSB for $\text{LiNi}_{0.5}\text{Mn}_{1.5}\text{O}_4$ -based cells in practical application. However, the aged TMSPi-containing electrolyte is unable to provide a protective effect on $\text{LiNi}_{0.5}\text{Mn}_{1.5}\text{O}_4$ due to the consumption of LiPF_6 and TMSPi accompanied by side reaction, resulting in inferior cyclic stability than cells in TMSB-containing electrolyte, as shown in Fig.S8. Therefore, the practitioner must offer a comprehensive evaluation from multiple perspectives in selecting suitable additives for practical application.

However, the high chemical reactivity of the selected additive may affect the thermal stability of

LiPF_6 -based electrolytes. Storage experiments are conducted with accelerated aging at 40 °C for four weeks. BE and TMSB-containing electrolytes can remain stable during storage. However, the TMSPi-containing electrolyte became cloudy after aging for weeks (Fig. 10a) and its ion conductivity decreased from 8.34 to 7.75 $\text{mS}\cdot\text{cm}^{-1}$ (Table S1). It may mainly ascribe to its spontaneous reaction with LiPF_6 , generating the insoluble of $(\text{Me}_3\text{SiO})\text{PF}_2$ and $(\text{Me}_3\text{Si})\text{POF}_2$ and increasing Li^+ diffusion obstruction with the consumption of LiPF_6 and TMSPi accompanied by this side reaction^[23,37]. As shown in Fig. 10a, the reactions between TMSPi and LiPF_6 can release more energy ($-314.33 \text{ kJ}\cdot\text{mol}^{-1}$) than TMSB ($-265.69 \text{ kJ}\cdot\text{mol}^{-1}$), suggesting TMSPi had a high chemical reactivity in LiPF_6 -based electrolyte. Based on the aged TMSPi-containing electrolyte after storage at 40 °C, the cells display relatively inferior cycling stability than that in TMSB-containing electrolyte, indicating that the consumption of TMSPi cannot support enough protection for high voltage cathode. Therefore, TMSPi displayed a lifetime limit as the additive in LiPF_6 -based electrolyte for high voltage electrodes. It is necessary to keep the TMSPi-containing electrolyte fresh for considerable evaluation and application.

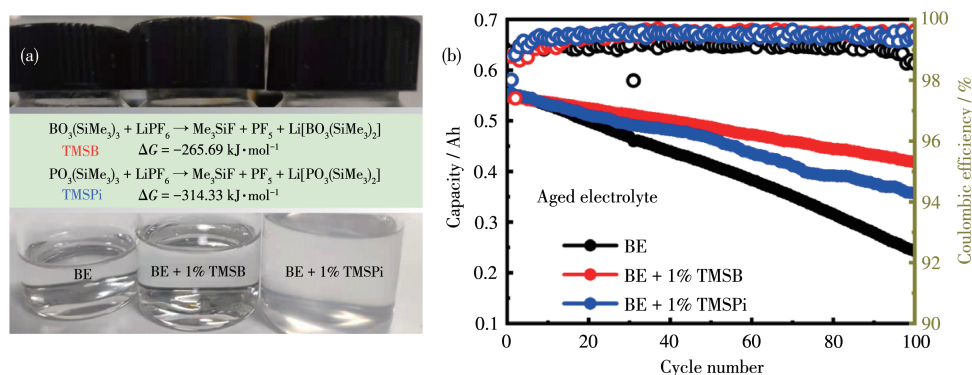


Fig.10 (a) Change of electrolytes after being stored at 40 °C for four weeks and reactivity; (b) Cycle performance of 0.5 Ah pouch cells at 1C in aged BE and additive-containing electrolytes for two weeks at 40 °C

3 Conclusions

TMSB or TMSPi as the selected additive was devoted to supporting $\text{LiNi}_{0.5}\text{Mn}_{1.5}\text{O}_4$ for practical application. Their effects on high voltage cathode and graph-

ite anode were systematically studied. Both two selected additives can be preferentially oxidized, participating in the formation of an interface layer on high voltage cathodes, resulting in enhanced Coulombic efficiency and cyclic stability of $\text{LiNi}_{0.5}\text{Mn}_{1.5}\text{O}_4$. Moreover, the

theoretical calculation suggests that the Si—O groups in TMSB or TMSPi, especially for TMSPi, can act as the HF scavenger in LiPF₆-based electrolytes. Significantly for TMSB, its electron-withdrawing atoms of B can act as the stabilizer of LiPF₆. TMSPi with higher HOMO value can rapidly passivate the surface of LiNi_{0.5}Mn_{1.5}O₄ and reduce the initial cell polarization, leading to superior electrochemical performance for LiNi_{0.5}Mn_{1.5}O₄ based cells. Moreover, TMSPi is likely to form an association with Li⁺ in the presence of EC and participate in the formation of the SEI layer on graphite electrodes via O—Si band cleavage. As a result, Graphite||LiNi_{0.5}Mn_{1.5}O₄ pouch cells with TMSPi-containing electrolyte displayed capacity retention of 88.9% after 100 cycles at 1C. However, TMSPi displayed a certain lifetime limit in LiPF₆-based electrolytes for its high chemical reactivity.

Acknowledgments: This work was financially supported by the National Natural Science Foundation of China (Grants No.21805186, 21625304, 21733012), the Shanghai Rising-Star Program (Grant No.20QB1401700), and the Technology Commission of Shanghai Municipality (Grant No.19160760700).

Supporting information is available at <http://www.wjhxxb.cn>

References:

- [1]Choi J W, Aurbach D. Promise and Reality of Post-Lithium-Ion Batteries with High Energy Densities. *Nat. Rev. Mater.*, **2016**,**1**(4):16013
- [2]Clark J M, Nishimura S, Yamada A, Islam S. High-Voltage Pyrophosphate Cathode: Insights into Local Structure and Lithium-Diffusion Pathways. *Angew. Chem. Int. Ed.*, **2012**,**51**(52):13149-13153
- [3]Fergus J W. Recent Developments in Cathode Materials for Lithium Ion Batteries. *J. Power Sources*, **2010**,**195**(4):939-954
- [4]赵江辉, 谢茂玲, 张海洋, 易若玮, 胡晨吉, 康拓, 郑磊, 崔瑞广, 陈宏伟, 沈炎宾, 陈立桅. 物理化学学报, **2021**,**37**(12):2104003
ZHAO J H, XIE M X, ZHANG H Y, YI R W, HU C J, KANG T, ZHENG L, CUI R G, CHEN H W, SHEN Y B, CHEN L W. *In Situ* Modification Strategy for Development of Room-Temperature Solid-State Lithium Batteries with High Rate Capability. *Acta Phys.-Chim. Sin.*, **2021**,**37**(12):2104003
- [5]郭峰, 陈鹏, 康拓, 王亚龙, 刘承浩, 沈炎宾, 卢威, 陈立桅. 负载纳米硅的锂-碳复合微球作为锂二次电池负极. 物理化学学报, **2019**,**35**(12):1365-1371
GUO F, CHEN P, KANG T, WANG Y L, LIU C H, SHEN Y B, LU W, CHEN L W. Silicon-Loaded Lithium-Carbon Composite Microspheres as Lithium Secondary Battery Anodes. *Acta Phys.-Chim. Sin.*, **2019**,**35**(12):1365-1371
- [6]Zhang L H, Min F Q, Luo Y, Dang G J, Gu H T, Dong Q Y, Zhang M H, Sheng L M, Shen Y B, Chen L W, Xie J Y. Practical 4.4 V Li||NCM811 Batteries Enabled by a Thermal Stable and HF Free Carbonate-Based Electrolyte. *Nano Energy*, **2022**,**96**:107122
- [7]Sun Z Y, Zhou H B, Luo X H, Che Y X, Li W S, Xu M Q. Design of a Novel Electrolyte Additive for High Voltage LiCoO₂ Cathode Lithium-Ion Batteries: Lithium 4 - Benzonitrile Trimethyl Borate. *J. Power Sources*, **2021**,**503**:230033
- [8]Li H H, Jin J, Wei J P, Zhou Z, Yan J. Fast Synthesis of Core-Shell LiCoPO₄/C Nanocomposite via Microwave Heating and Its Electrochemical Li Intercalation Performances. *Electrochem. Commun.*, **2009**, **11**(1):95-98
- [9]Hu M, Tian Y, Su L W, Wei J P, Zhou Z. Preparation and Ni-Doping Effect of Nanosized Truncated Octahedral LiCoMnO₄ as Cathode Materials for 5 V Li-Ion Batteries. *ACS Appl. Mater. Interfaces*, **2013**,**5** (22):12185-12189
- [10]Hu M, Tian Y, Wei J P, Wang D G, Zhou Z. Porous Hollow LiCoMnO₄ Microspheres as Cathode Materials for 5 V Lithium Ion Batteries. *J. Power Sources*, **2014**,**247**:794-798
- [11]Hu M, Pang X L, Zhou Z. Recent Progress in High-Voltage Lithium Ion Batteries. *J. Power Sources*, **2013**,**237**:229-242
- [12]Zhou L, Zhao D, Lou X. LiNi_{0.5}Mn_{1.5}O₄ Hollow Structures as High-Performance Cathodes for Lithium-Ion Batteries. *Angew. Chem. Int. Ed.*, **2012**,**51**(1):239-241
- [13]Shin D W, Manthiram A. Surface-Segregated, High-Voltage Spinel LiMn_{1.5}Ni_{0.42}Ga_{0.08}O₄ Cathodes with Superior High-Temperature Cyclability for Lithium-Ion Batteries. *Electrochem. Commun.*, **2011**, **13**(11):1213-1216
- [14]Marom R, Amalraj S F, Leifer N, Jacob D, Aurbach D. A Review of Advanced and Practical Lithium Battery Materials. *J. Mater. Chem.*, **2011**,**21**(27):9938-9954
- [15]Lee H, Han T, Cho K Y, Ryou M H, Lee Y M. Dopamine as a Novel Electrolyte Additive for High-Voltage Lithium-Ion Batteries. *ACS Appl. Mater. Interfaces*, **2016**,**8**(33):21366-21372
- [16]Park O K, Cho Y, Lee S, Yoo H, Song H, Cho J. Who Will Drive Electric Vehicles, Olivine or Spinel? *Energy Environ. Sci.*, **2011**,**4**(5): 1621-1633
- [17]Kraetsberg A, Ein-Eli Y. Higher, Stronger, Better... A Review of 5 Volt Cathode Materials for Advanced Lithium-Ion Batteries. *Adv. Energy Mater.*, **2012**,**2**(8):922-939
- [18]Xia J, Sinha N N, Chen L P, Kim G Y, Xiong D J, Dahn J R. Study of Methylene Methanedisulfonate as an Additive for Li-Ion Cells. *J. Electrochem. Soc.*, **2013**,**161**(1):84-88
- [19]Dumaz P, Rossignol C, Mantoux A, Sergent N, Bouchet R. Kinetics Analysis of the Electro-catalyzed Degradation of High Potential LiNi_{0.5}Mn_{1.5}O₄ Active Materials. *J. Power Sources*, **2020**,**469**:228337
- [20]Zou Z Y, Xu H T, Zhang H R, Tang Y, Cui G L. Electrolyte Therapy for Improving the Performance of LiNi_{0.5}Mn_{1.5}O₄ Cathodes Assem-

- bled Lithium-Ion Batteries. *ACS Appl. Mater. Interfaces*, **2020**,**12**(19): 21368-21385
- [21] Liao X L, Huang Q H, Mai S W, Wang X S, Xu M Q, Xing L D, Liao Y H, Li W S. Self-Discharge Suppression of 4.9 V $\text{LiNi}_{0.5}\text{Mn}_{1.5}\text{O}_4$ Cathode by Using Tris(trimethylsilyl)borate as an Electrolyte Additive. *J. Power Sources*, **2014**,**272**:501-507
- [22] Rong H B, Xu M Q, Xie B Y, Liao X L, Huang W Z, Xing L D, Li W S. Tris(trimethylsilyl)borate (TMSB) as a Cathode Surface Film Forming Additive for 5V $\text{Li}/\text{LiNi}_{0.5}\text{Mn}_{1.5}\text{O}_4$ Li-Ion Cells. *Electrochim. Acta*, **2014**,**147**:31-39
- [23] Guéguen A, Bolli C, Mendez M A, Berg E J. Elucidating the Reactivity of Tris(trimethylsilyl) phosphite and Tris(trimethylsilyl)phosphate Additives in Carbonate Electrolytes—A Comparative Online Electrochemical Mass Spectrometry Study. *ACS Appl. Mater. Interfaces*, **2019**,**3**(1):290-299
- [24] Liao X L, Zheng X W, Chen J W, Huang Z Y, Xu M Q, Xing L D, Liao Y H, Lu Q L, Li X F, Li W S. Tris(trimethylsilyl)phosphate as Electrolyte Additive for Self-Discharge Suppression of Layered Nickel Cobalt Manganese Oxide. *Electrochim. Acta*, **2016**,**212**:352-359
- [25] Yan G C, Li X H, Wang Z X, Guo H J, Wang C. Tris(trimethylsilyl) phosphate: A Film-Forming Additive for High Voltage Cathode Material in Lithium-Ion Batteries. *J. Power Sources*, **2014**,**248**:1306-1311
- [26] Rong H B, Xu M Q, Xing L D, Li W S. Enhanced Cyclability of $\text{LiNi}_{0.5}\text{Mn}_{1.5}\text{O}_4$ Cathode in Carbonate Based Electrolyte with Incorporation of Tris(trimethylsilyl)phosphate (TMSP). *J. Power Sources*, **2014**,**261**:148-155
- [27] Mai S W, Xu M Q, Liao X L, Hu J N, Lin H B, Xing L D, Liao Y H, Li X P, Li W S. Tris(trimethylsilyl)phosphite as Electrolyte Additive for High Voltage Layered Lithium Nickel Cobalt Manganese Oxide Cathode of Lithium Ion Battery. *Electrochim. Acta*, **2014**,**147**:565-571
- [28] Wang Y T, Xing L D, Li W S, Bedrov D. Why Do Sulfone-Based Electrolytes Show Stability at High Voltages? Insight from Density Functional Theory. *J. Phys. Chem. Lett.*, **2013**,**4**(22):3992-3999
- [29] Han Y K, Yoo J, Yim T. Why is Tris(trimethylsilyl)phosphite Effective as an Additive for High-Voltage Lithium-Ion Batteries? *J. Mater. Chem. A*, **2015**,**3**(20):10900-10909
- [30] Song Y M, Kim C K, Kim K E, Hong S Y, Choi N S. Exploiting Chemically and Electrochemically Reactive Phosphite Derivatives for High-Voltage Spinel $\text{LiNi}_{0.5}\text{Mn}_{1.5}\text{O}_4$ Cathodes. *J. Power Sources*, **2016**,**302**:22-30
- [31] Yoon T, Park S, Mun J, Ryu J H, Choi W, Kang Y S, Park J H, Oh S M. Failure Mechanisms of $\text{LiNi}_{0.5}\text{Mn}_{1.5}\text{O}_4$ Electrode at Elevated Temperature. *J. Power Sources*, **2012**,**215**:312-316
- [32] Marchini F, Williams F J, Calvo E J. Electrochemical Impedance Spectroscopy Study of the $\text{Li}_x\text{Mn}_2\text{O}_4$ Interface with Natural Brine. *J. Electroanal. Chem.*, **2018**,**819**:428-434
- [33] Ma Y, Wang C D, Ma J, Xu G J, Chen Z, Du X F, Zhang S, Zhou X H, Cui G L, Chen L Q. Interfacial Chemistry of γ -Glutamic Acid Derived Block Polymer Binder Directing the Interfacial Compatibility of High Voltage $\text{LiNi}_{0.5}\text{Mn}_{1.5}\text{O}_4$ Electrode. *Sci. China Chem.*, **2021**, **64**(1):92-100
- [34] Wang K, Xing L D, Zhu Y M, Zheng X W, Cai D D, Li W S. A Comparative Study of Si-Containing Electrolyte Additives for Lithium Ion Battery: Which One is Better and Why is It Better. *J. Power Sources*, **2017**,**342**:677-684
- [35] Yim T, Han Y K. Tris(trimethylsilyl) Phosphite as an Efficient Electrolyte Additive to Improve the Surface Stability of Graphite Anodes. *ACS Appl. Mater. Interfaces*, **2017**,**9**(38):32851-32858
- [36] Zaghbi K, Mauger A, Groult H, Goodenough J B, Julien C M. Advanced Electrodes for High Power Li-Ion Batteries. *Materials*, **2013**,**6**(3):1028-1049
- [37] Qi X, Tao L, Hahn H, Schultz C, Gallus D R, Cao X, Nowak, Röser S, Li J, Laskovic I C, Rad B R, Winter M. Lifetime Limit of Tris(trimethylsilyl)phosphite as Electrolyte Additive for High Voltage Lithium Ion Batteries. *RSC Adv.*, **2016**,**6**(44):38342-38349